HiSST: 3rd International Conference on
High-Speed Vehicle Science Technology
14 -19 April 2024, Busan, Korea

Drag due to distributed roughness in supersonic turbulent boundary layers: comparison between experiments and numerics

Q. Chanzy[1], S. Morilhat[2], A. Durant[1], V. Brion[2]

Abstract

The purpose of this paper is to present the design of a test bench installed in the ONERA R1Ch blow down wind tunnel and the subsequent test campaign conducted in an effort to measure the drag increment due to a rough surface in a supersonic flow. Distributed roughnesses of size from ~1µm to 65µm, generated by commercial sand papers, have been tested. Reynolds Averaged Navier Stokes simulations of the flow have been conducted accounting for these roughnesses through a roughness correction model. The numerical and experimental results are compared and the link between the size of the roughness and the equivalent sand grain roughness is discussed.

Keywords: *Supersonic flow, turbulent boundary layer, roughness, experimental, RANS*

Nomenclature

Latin
ks – Equivalent sand grain
Fx – Longitudinal shear stress
dFx – Uncertainty of longitudinal shear stress
$dFSmooth$ – Difference of longitudinal shear stress with respect to the smooth sample
Pi – Stagnation pressure
Ra – Averaged roughness
Ti – Stagnation temperature
U – Flow velocity
y – Normal wall distance
Greek
κ – Von Karman constant
Superscripts
+ – Non dimensional variable
Subscripts
∞ – Rough regime

1. Conception of the test bench

1.1 Context

The challenging thermal environment encountered by high-speed vehicles calls for the development of new materials like composite or 3D printed metal, and better modelling capacities for their design. These materials feature a surface finish that is rougher than the metallic parts classically used. This challenges the accuracy of current simulation tools for accurate drag estimate. Efficient design of hypersonic vehicles thus requires the investigation of the drag impact of rough surfaces and improved models.

Roughnesses can have two impacts on boundary layers. It can trigger the laminar/turbulent transition and it can increase the wall shear stress in comparison with a smooth wall. This paper deals with the later effect in supersonic turbulent boundary layers.

There are various methods to take into account the impact of roughness on wall shear stress in numerical calculations [1, 2]. These methods mostly find their roots in Nikuradse's study on rough regime in pipe flows [4]. Nikuradse suggested that in a fully rough regime, the impact of the roughness

[1] *MBDA, 1 avenue Réaumur, 92358 Le Plessis-Robinson CEDEX, France , quentin.chanzy@mbda-systems.com*
[2] *DAAA, ONERA Université Paris Saclay F-92190 Meudon France*

may be modelled as a shift ΔU^+ in the logarithmic region of the boundary layer. This impact is illustrated in Fig 1. The classical and modified logarithmic laws are presented in Eq.(1 and 2.

$$U^+(y) = \kappa^{-1} log\ y^+ + A \quad \textbf{(1)}$$

$$U^+(y) = \kappa^{-1} log\ y^+ + A - \Delta U^+ \quad \textbf{(2)}$$

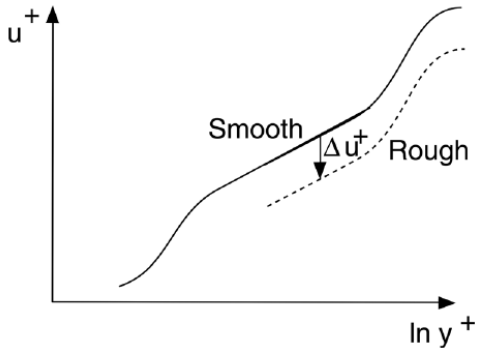

Fig 1: Impact of roughness on velocity profile in the boundary layer, in wall units, taken from [1]

Following this work, Schilchting [3] proposed the definition of a physical quantity ks_∞ called equivalent sand grain, which characterizes the impact of the surface roughness on the flow, based on the main roughness parameters: averaged height, density, distribution and shape. This equivalent grain of sand can then be used to construct a rough Reynolds number $k_{s\infty}^+$ of the flow, which, in turn, can characterize the rough regime cf. Fig 2 :

- A first regime for $k_{s\infty}^+ \sim < 4$ said "aerodynamically smooth" regime for which the flow is similar to a flow on a smooth plate $\Delta U^+ \sim 0$.
- A purely rough regime $k_{s\infty}^+ \sim > 68$ for which the viscous effects are negligible compared with the pressure drag, the correction then does not depend on the nature of the roughness, the impact of roughness on the logarithmic law relates directly to the Reynolds number ks_∞^+ [3].
- A transient regime ("mistakenly" named transition regime – there is absolutely no connection with the phenomenon of laminar/turbulent transition) during which the correction depends on parameters other than the ks_∞.

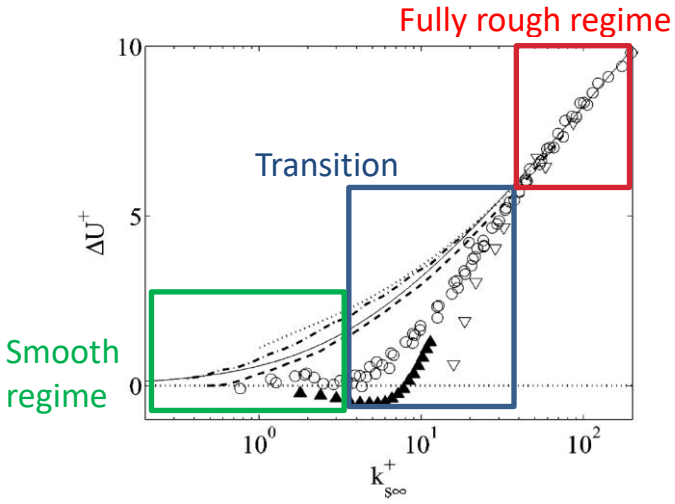

Fig 2 : Correction of the logarithmic law of the turbulent boundary layer as a function of the roughness Reynolds number for different experimental works (adapted from [2]).

Several studies have been conducted to find a universal law linking a material roughness's characteristics and its equivalent sand grain. Bons [12] conducted a comprehensive literature review on that subject and concluded upon the difficulty of finding such a universal law. For the specific domain of high supersonic / hypersonic flows, investigations and results are also scarce.

In order to be able to measure the impact of roughnesses on drag and thus the equivalent grain sand of these materials, a test bench, presented on Fig 4, has been conceived and tested in the R1Ch ONERA blow down wind tunnel.

2. Experimental setup

2.1. Wind tunnel

The R1Ch wind tunnel is a supersonic cold blow down facility located at ONERA Meudon centre [5,6] with possible operation at Mach 3 and 5. Here the Mach number is set to 3 and the stagnation pressure and temperature were nominally 10 bar and 300 K, respectively. This results in a unit Reynolds number of 80 million.m^{-1}. Other tests were performed at 5 and 15 bar corresponding to a unit Reynolds number of 40 million.m^{-1} and 120 million.m^{-1}.

2.2. Test bench

A test bench has been designed for this wind tunnel, to measure the drag induced by roughnesses. The operating principle is presented on Fig 3. The main assembly consists of a samples holder and two samples of rough surfaces placed symmetrically, one positioned above and one below in order to double the drag measurement and increase accuracy. This specimen holder makes it possible, with the aid of weakened arms, to completely absorb the transverse and normal forces imposed by the airflow that are principally expected to occur when the flow starts and unstarts at the beginning and end of the blow down process. On the contrary, the mechanical system almost completely transfers the longitudinal drag force to the Kistler 9215A sensor placed at the rear of the mounting system.

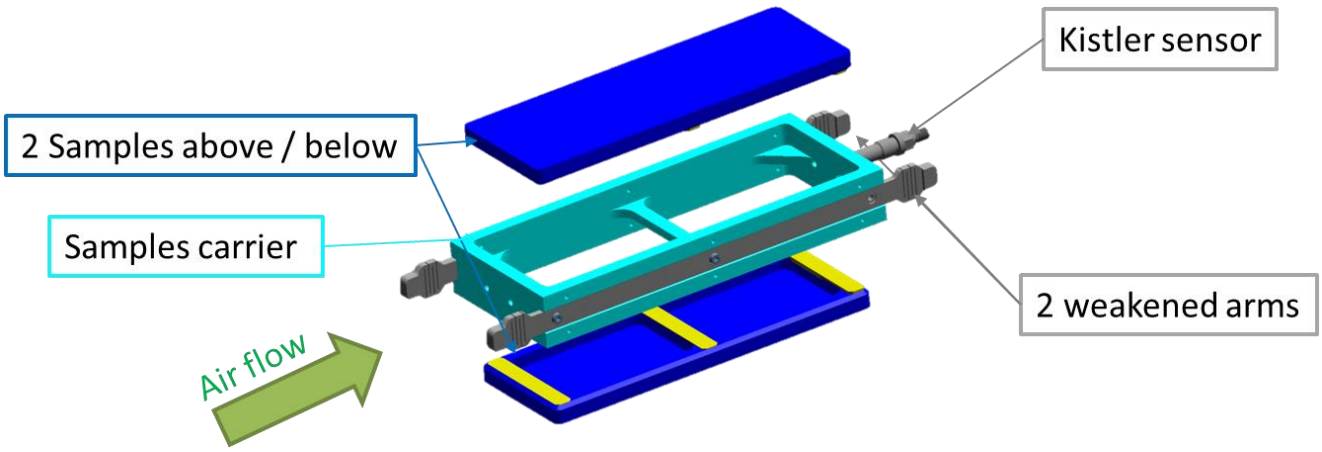

Fig 3: Schematic diagram of the axial force measurement device.

This assembly is mounted on a base which is positioned in the Mach rhombus of the wind tunnel. The base nose is a symmetric wedge of 10° total angle that divides the flow symmetrically above and below. This angle ensures that the shockwaves are attached to the tip of the wedge, thus flow conditions are uniform along the wedge. The lengths of the wedge and the sample was chosen such as the flow above the middle of the samples is also uniform. For an upstream Mach 3 flow, the stagnation pressure drop through the shockwaves is such as the Mach number above the samples is above Mach 2.97.
The alignment of the model with the flow is adjusted by means of the differential pressure sensor placed upstream of the sample holder. A lever arm mounting and calibrated weights are provided to calibrate the axial force measurement device by disassembling only the samples. This calibration also

permitted to confirm the mechanical design of the weakened arms: more than 90% of the drag force is recovered by the Kistler sensor.

The bench equipped with rough samples is visible in the test section of the R1Ch wind tunnel on Fig 4.

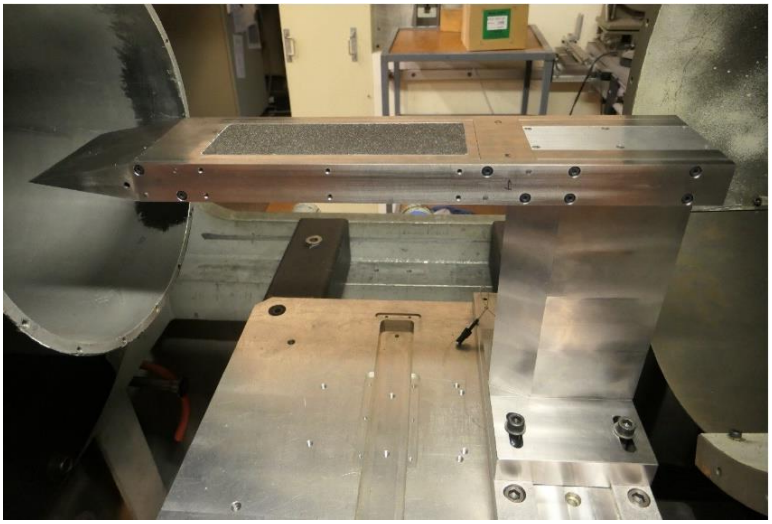

Fig 4. Photography of the test bench equipped with the P80 samples in the R1Ch wind tunnel.

2.3. Test samples

Regular sand papers have been used as test samples, to achieve various roughness Reynolds numbers. A selection of sand papers was measured using a MarSurf M400 profilometer, and three of them were then sub-selected for the wind tunnel tests. Their arithmetic average roughness Ra is presented in Table 1.

Table 1. : Roughness properties of the different samples.

Sample	Ra [µm]
Smooth	0.4
P1000	6.0
P240	17.5
P80	65.2

2.4. Test program

The test program is displayed in Table 2.
It is designed to study three different effects:

- The effect of roughness amplitude, with a variation of samples at a given stagnation pressure, with the stagnation temperature at minimum (300 K),
- The effect of stagnation pressure for the two samples at the extreme Ra, namely the Smooth one and the P80 one. These two samples were tested at stagnation pressure of 5, 10, and 15 bar.
- The effect of stagnation temperature on the Smooth sample at 5, 10 and 15 bar.

Table 2 : Test program

Study	Pi [bar]	Ti [K]	Sample
Roughness	10	300	Smooth
			P80
			P240
			P1000
Stagnation pressure	5		Smooth
	15		
	5		P80
	15		
Stagnation temperature	5	330	Smooth
	10		
	15		

2.5. Thermal effect

The first wind tunnel runs indicated that the drag measurement, assumed to be constant once the flow is established, drifts temporally at a constant rate. This is due to the mechanical constraint applied upon the model under the flow aerothermal load, which either heats up or cools down the model, depending on the stagnation temperature of the freestream. Because of these temperature effects, the flanks of the model expand or contract, which modifies the stress applied upon the force sensor, on top of the axial force applied by the drag.

A correction of this effect was thus required. This was achieved by repeating the same test with a different stagnation temperature, for every stagnation pressure. Since the variation of stagnation temperature has little effect on the value of the drag force, the runs at the two different stagnation temperatures must reach the same value at some point of the measurement history. The right measurement therefore lies at the intersection of the two curves subjected to the drift. The value is practically obtained by taking the intersection of the linear regressions of the curves. The regression also helps improving the signal over noise ratio. The method is presented on Fig 5. The intersection time is 0.74 s and a variation of the interpolation zone of +-0.25 s further provides the measurement uncertainty.

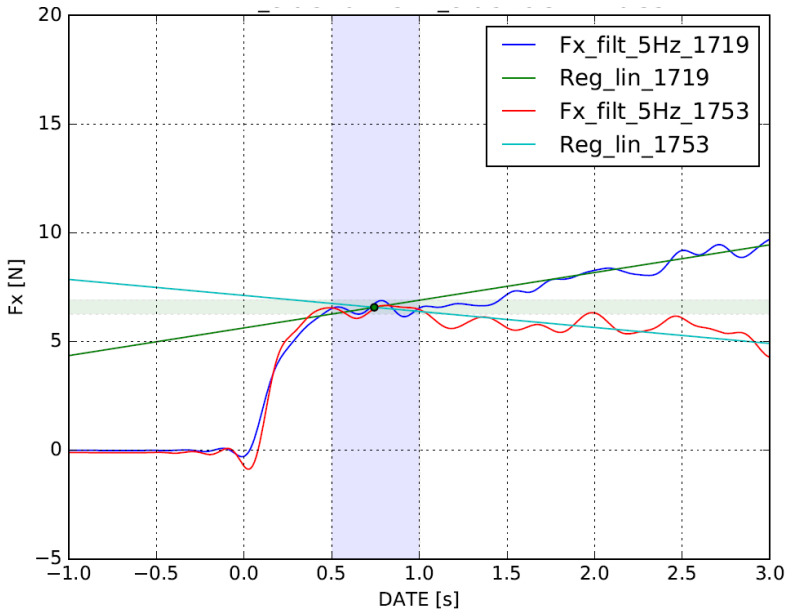

Fig 5: Method of determining the force measurement using two different Ti runs on the smooth sample at Pi 10bar (1719 300K, 1753 330K). $Fx = 6.6N + -0.3N$.

3. Results

The results of the tests are presented in Table 3. The drag increases with increased roughness and stagnation pressure, as expected. These values are further discussed in paragraph 5, in comparison with the results obtained by numerical simulations.

Table 3: Experimental values of the drag

Study	Pi [bar]	Ti [K]	Sample	Fx [N]	dFx [N]	$dFSmooth$ [N]
Roughness	10	300	Smooth	7.5	0.2	
			P80	18.4	0.3	10.9
			P240	11.6	0.4	4.1
			P1000	8.3	0.3	0.8
Stagnation pressure	5		Smooth	3.9	0.1	
	15			8.4	0.6	
	5		P80	6.2	0.1	2.3
	15			26.8	0.5	18.4

4. Numerical calculations

One of the goals is to evaluate the ability of the CFD code CEDRE [12] to match the effect of roughness on drag found experimentally and to search for a relationship between $k_{s\infty}$ and Ra. Several calculations were realized, with the main parameters described below.

The calculations use a 3D model of the flow to account for the secondary flow effects, mainly at the side of the model. The oil flow visualizations displayed in Fig 6 show that the flow is strongly 3D at the upper surface of the sample with a divergence and then convergence of the friction lines.

The numerical model uses a completely unstructured mesh, as presented in Fig 7. The refined mesh at the level of the two samples is composed of 65 million elements with $y^+ < 1$ at the wall and a geometric progression of ratio 1.06 for the prism mesh of the boundary layer.

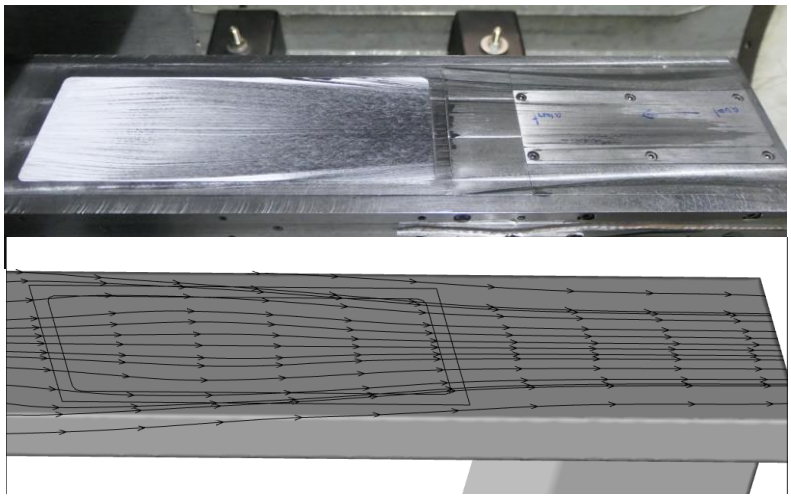

Fig 6: Visualization of the friction lines by colored oil in the wind tunnel and on a 3D calculation

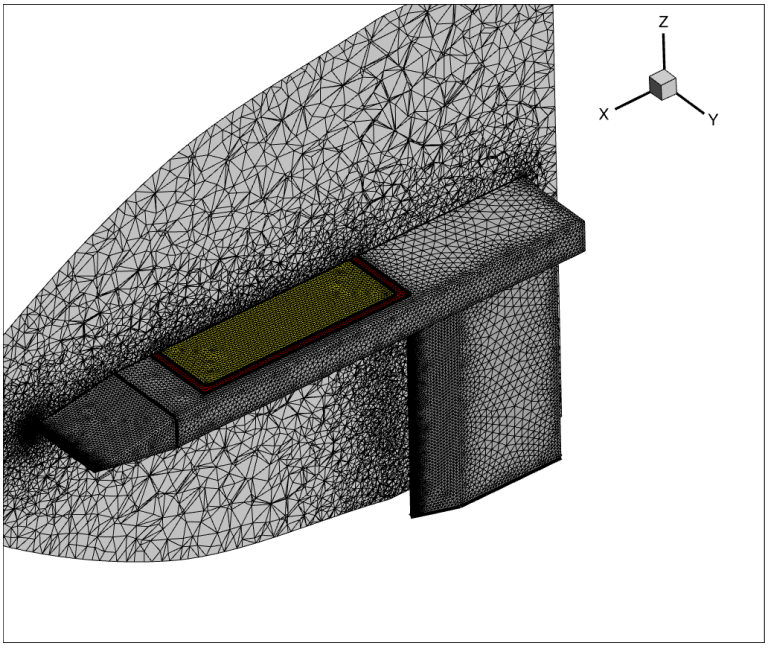

Fig 7: Surface Mesh and Longitudinal Section. Sample (yellow) and sample holder (red).

Calculations are performed using a Reynolds Average Navier Stokes (RANS) method, the turbulence being modelled by the K-omega SST model and the roughness by the Aupoix 2015 model [1]. The CFD solver uses a cell-centered finite volume method. The spatial and time integrations are carried out using an Advection Upstream Splitting Method Plus (AUSM+) and an implicit scheme solved with generalized minimal residual method (GMRES) iterations, respectively. The boundary conditions are: adiabatic walls for the bench with the corresponding roughness parameters on the samplings, supersonic inflow at stagnation conditions for the far field and supersonic outflow downstream of the bench. The calculations are converged up to variation of less than 0.002N on the drag force on the samples.

The relationship between the average roughness and the equivalent grain of sand is initially chosen as:

$$\boldsymbol{ks_{\infty} = 12.5 * Ra} \qquad \textbf{(3)}$$

This expression follows the work of Hue et al. [12].

The sharp increase in wall shear stress on the sample due to the roughness is visible in Fig 8 which compares a 3D visualization of the flow on the model for the smooth case and the roughest case, P80. It may be noted that the boundary layer is modified by the roughness, as can be seen from the Mach field. On the contrary the friction lines are not affected by the increased roughness.

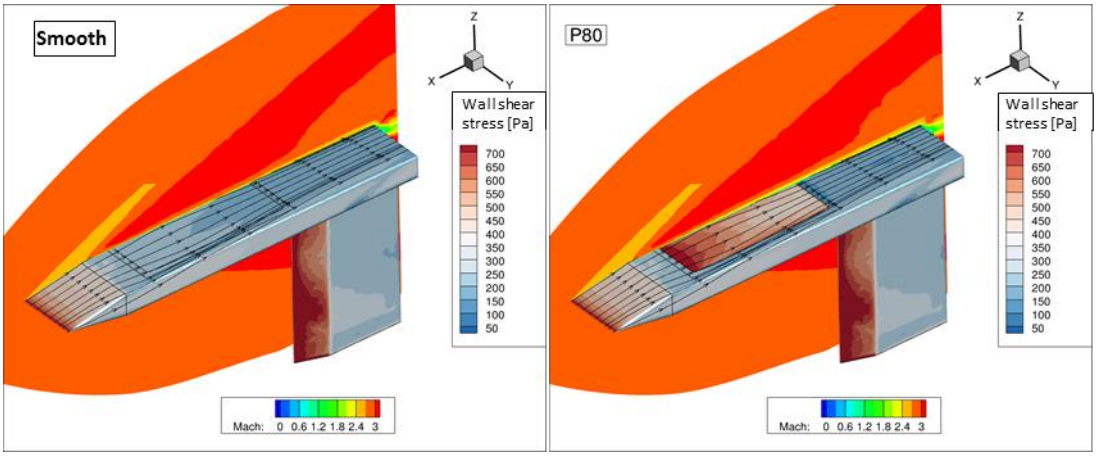

Fig 8: Visualization of friction on the Smooth and P80 samples, and of the Mach field on an XZ plane.

Fig 9 shows the wall shear stress on the same samples and compares the wall shear stress field on the top and bottom samples. The fields are generally similar. It can be noted that there is no impact of the mast holding the model on the bottom sample. Hence the flow exhibits a good up and down symmetry, which is a prerequisite for a proper measurement of the axial force. This hypothesis was also confirmed experimentally using schlieren measurements.

All the calculations performed and their results are presented in Table 4.
The small differences in stagnation pressure and temperature with the experimental tests are due to experimental difficulties to reach precisely enough the target conditions. Nevertheless, the thermal effect is negligible in terms of drag, as it can be seen in Table 4. And the stagnation pressure difference only occurs on the case at 14.8bar. The difference is only 1% of the stagnation pressure and considered negligible.

Table 4 : Parameters and results of the CFD calculations.

Study	Pi [bar]	Ti [K]	Sample	Ra[µm]	ks_∞[µm]	Fx [N]	$dFSmooth$ [N]
Roughness	10	280	Smooth	0.4	0.	7.8	
			P80	65.2	815.	17.8	10.0
			P240	17.5	194.	13.9	6.1
			P1000	6.0	75.	11.8	4.0
Stagnation pressure	5		Smooth	0.4	0.	4.5	
	14.8			0.4	0.	10.8	
	5		P80	65.2	815.	9.3	4.8
	14.8			65.2	815.	26.1	15.3
Stagnation temperature	10	310	Smooth	0.4	0.	7.9	0.1 (vs Smooth 280K)

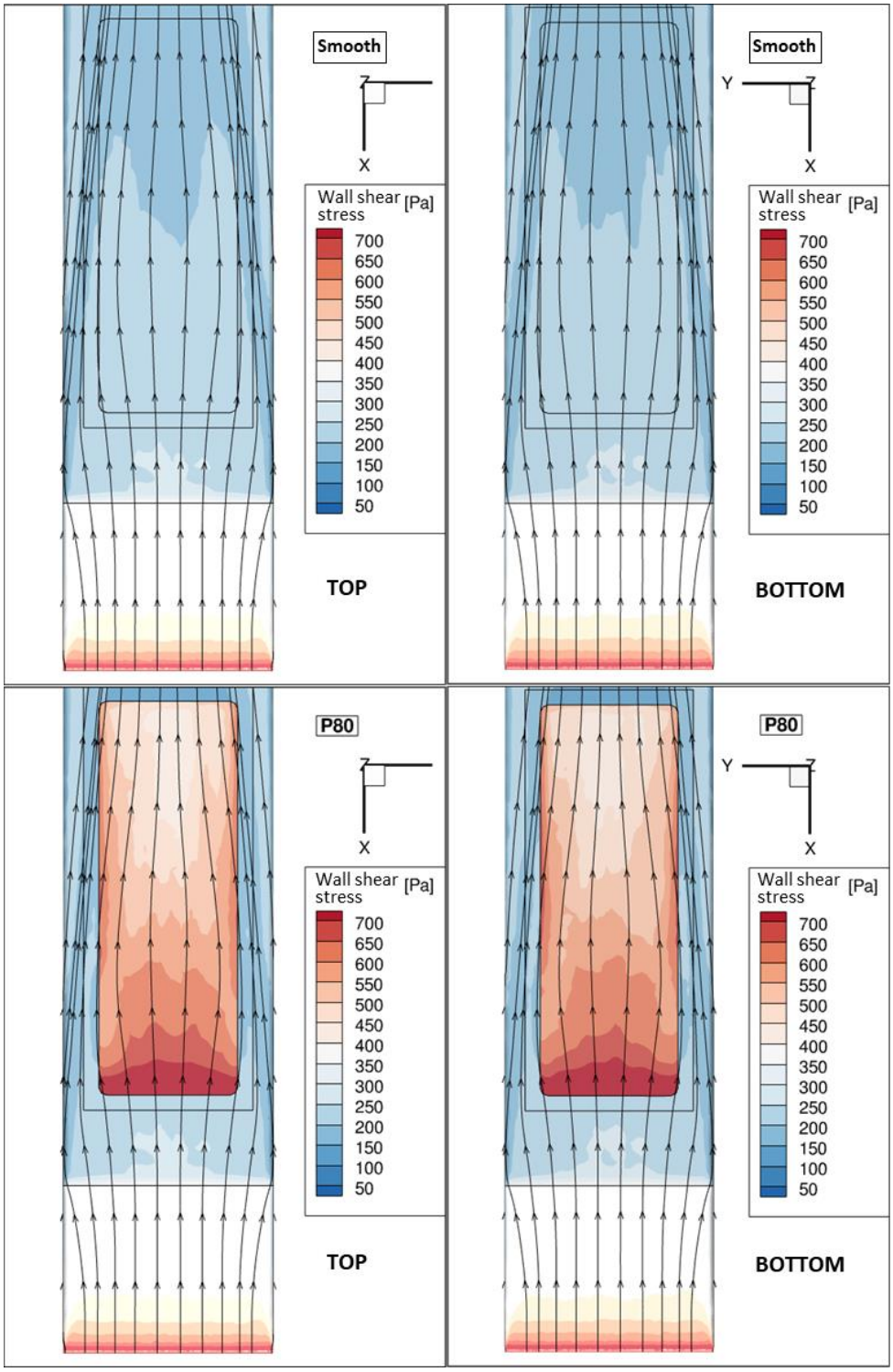

Fig 9: Visualization of the friction lines and wall shear stress fields on the smooth top/bottom and P80 samples

The calculations are divided into 3 categories: a roughness effect, a stagnation pressure effect and a stagnation temperature effect. The stagnation temperature effect analysis validates that stagnation temperature variation do not modify the longitudinal drag force but only heats up or cools down the model. The effects of stagnation pressure and roughness allow drawing comparisons with the experimental results.

5. Comparison of numerical calculations / experimental measurements:

Numerical calculations and experimental measurements of the roughness effect are compared in **Fig 10**. The measurements of the force are very similar to the CFD model for the smooth case and the roughest case, P80. These results validate the measurement method for the smooth case and the roughness model for the rough case.

In contrast, for the less rough P1000 and P240 samples, there is a large difference between the experimental and the numeric, with the numeric overestimating the effect of roughness on drag. This may be due to two main causes which cannot be separated with a single measurement: a different correlation between ks_∞ and Ra or a flow not in a fully rough regime, but in the transition regime (cf. Fig 2). Measurements at higher Reynolds should be repeated to clearly detect the change in regime and thus define the ks_∞ equivalent sand grain for these levels of roughness.

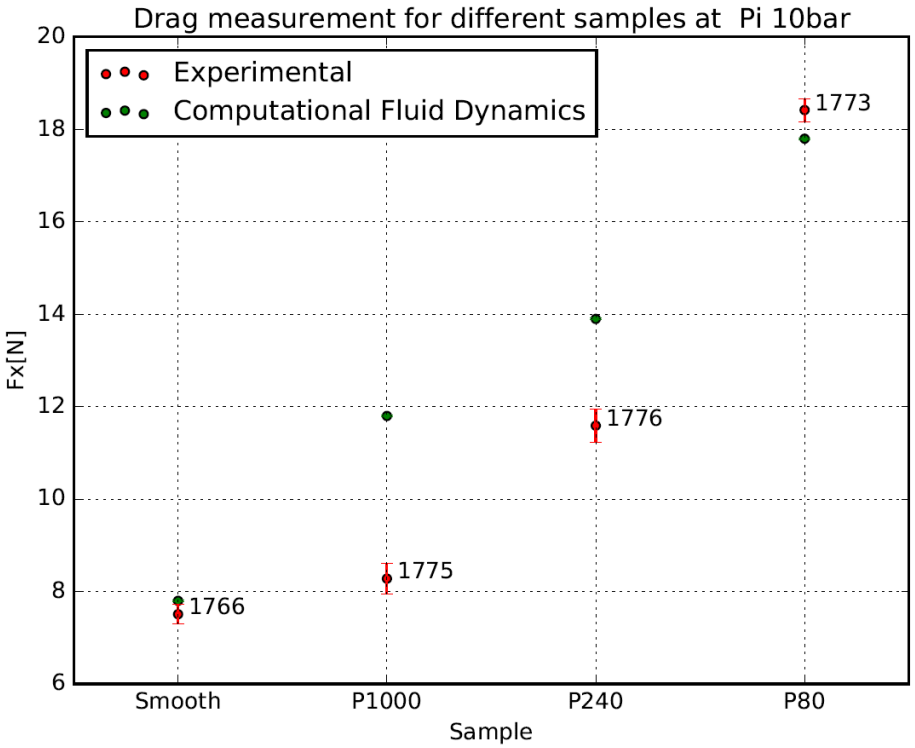

Fig 10: CFD / experimental drag comparisons, roughness effect.

Fig 11 presents the results of the stagnation pressure effect, and thus of Reynolds, on the smooth and P80 samples. For the smooth case, the numerical and experimental match. It can be noted that the three measurements at 15 bars are slightly dispersed on the smooth sample, which is due to a requirement of more complicated adjustment on the settings of the wind tunnel for these runs.

In the P80 case, the method is consistent for 10 and 15 bar, but diverges at 5 bar. This 5 bar gap may be due to a Reynolds number too low to be in the fully rough regime. Again, the numeric over-predicts drag. It may be advisable to repeat this measurement to confirm this discrepancy.

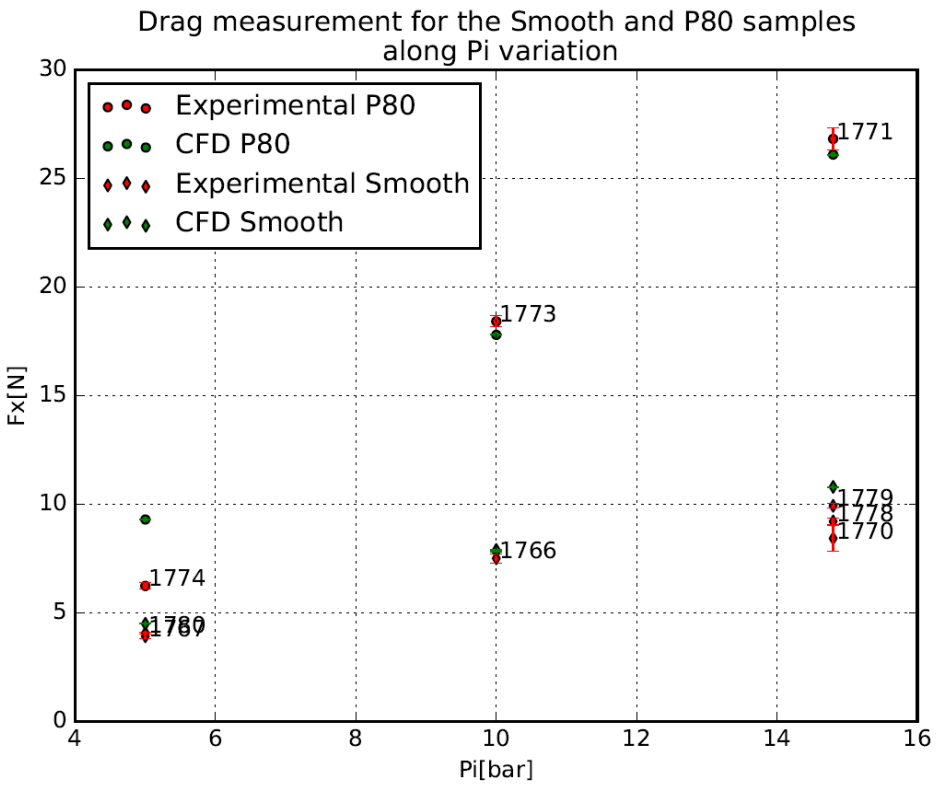

Fig 11: CFD / experimental drag comparison, stagnation pressure effects.

6. Conclusion

A new test bench at ONERA R1Ch blow down wind tunnel dedicated to wall shear stress measurement in a supersonic flow made it possible to validate the method of measuring drag induced by roughnesses of various sizes at a high Mach number of 3. The numerical / experimental comparisons validate the approach and the equivalent sand grains approach.

The teachings from this work are:

- Thermal effect can play a first order role on the test bench measurements,
- The CFD modelling method of the impact of roughness is validated,
- The Reynolds number should be varied widely to ensure the measurements in the fully rough regime,
- The relationship between ks_∞, an equivalent sand grain and Ra, needs to be measured in a wind tunnel. It does not seem universal (as already reported in the literature).

Future test campaigns will be held in the R1Ch wind tunnel in order to improve the understanding of the relationship between other roughness parameters and equivalent sand grains. High Mach number runs will also be made in the R2Ch wind-tunnel.

References

- Journal article

1. Aupoix, B.: Roughness corrections for the k–ω shear stress transport model: Status and proposals. Journal of Fluids Engineering 137.2 (2015)
2. Jiménez, J.: Turbulent flows over rough walls. *Annu. Rev. Fluid Mech.* 36 (2004)
3. Schlichting, H.: Experimentelle untersuchungen zum rauhigkeitsproblem. *Ingenieur-Archiv* 7.1 (1936)

4. Nikuradse, J.: Laws of flows in rough pipes. Washington: NACA. (1937)
5. Papirnyk, O., et al. : Conception et qualification de la soufflerie silencieuse R1Ch de l'ONERA. *Aerodynamics of Wind Tunnel Circuits and their Components* (1997)
6. Chanetz, B et al (2020). *Experimental Aerodynamics*. Springer International Publishing.
7. Bons, J P. : A review of surface roughness effects in gas turbines. (2010): 021004.
8. Hue, D. et al. : Turbulent drag induced by low surface roughness at transonic speeds: Experimental/numerical comparisons. *Physics of Fluids* 32.4 (2020).
9. Refloch, A., et al. : CEDRE software. *Aerospace Lab* 2 (2011)